electronics

MDPI

Article

Improvement of UAV Tracking Technology in Future 6G Complex Environment Based on GM-PHD Filter

Tao Hong [1,2,3], Chunying Zhou [1,*], Michel Kadoch [4], Tao Tang [1] and Zhengfa Zuo [5]

[1] School of Electronic and Information Engineering, Beihang University, Beijing 100191, China
[2] Shenzhen Institute of Beihang University, Shenzhen 518063, China
[3] Yunnan Innovation Institute·BUAA, Kunming 650233, China
[4] École de Technologie Supérieure (ETS), University of Quebec, Montreal, QC H3C 1K3, Canada
[5] QuakeSafe Technologies Co., Ltd., Kunming 650100, China
* Correspondence: zy2102127@buaa.edu.cn; Tel.: +86-152-3690-0531

Abstract: Unmanned aerial vehicles (UAVs) will become an indispensable part of future sixth-generation (6G)-based mobile networks that can provide flexible deposition, strong adaptability, and high service quality. Under the guarantee of blockchain, UAVs can provide efficient communication or computing services for ground intelligence devices and promote the development of wireless communication. However, as the number of UAVs increases, issues regarding UAV path planning, the handling of emergencies, the intrusion of illegal UAVs, etc., will need to be addressed. This paper proposes an improved Gaussian mixture probability hypothesis density (GM-PHD) filter based on machine learning for the target tracking and recognition of non-cooperative UAV swarms. Simulation results demonstrate that the improved filter can effectively suppress clutter interference in complex environments and improve the performance of multi-target recognition and trajectory tracking compared with the traditional GM-PHD filter.

Keywords: 6G; blockchain; GM-PHD filter; UAV tracking

Citation: Hong, T.; Zhou, C.; Kadoch, M.; Tang, T.; Zuo, Z. Improvement of UAV Tracking Technology in Future 6G Complex Environment Based on GM-PHD Filter. *Electronics* **2022**, *11*, 4140. https://doi.org/10.3390/electronics11244140

Academic Editor: Christos J. Bouras

Received: 10 November 2022
Accepted: 10 December 2022
Published: 12 December 2022

1. Introduction

1.1. Background

The evolution of sixth-generation (6G) communication technology has been advancing following the deployment of fifth-generation (5G) mobile networks around the world in 2019 [1]. This includes developments in the standard formulation and emerging technologies to meet the requirements of the current era. Sixth-generation technology will improve data rates, reliability, fast mobility, and network intelligence. A variety of smart community wireless communication infrastructures, such as transportation systems, power grids, and other systems, can also be improved with 6G as it facilitates the efficient processing of large amounts of data [2,3]. It is anticipated that 6G wireless network connections will continue to advance in maturity and dependability over time.

Unmanned aerial vehicles (UAVs), also called drones, are aerial robots that can fly on their own or under human control. UAVs have been recognized as an essential 6G communication technology due to their flexibility and ability to attain close proximity, which improves the quality of UAV applications [4,5]. In addition, as a decentralized, open, and transparent distributed ledger technology, blockchain technology can be tightly integrated with UAV communication. By offering a decentralized, safe, and reliable environment, UAV communication can achieve efficient, fast, and secure service delivery and provide a strong guarantee for the 6G network [6]. Under the 6G network envisioned by blockchain, UAV communication will facilitate multiple connectivity, service large coverage areas, contribute to different applications, and provide better service quality [7,8]. UAVs are flying machines that can also be used to easily capture and collect highly accurate data from multiple scenarios, including the land, sea, and air. During the dissemination process,

the data are transformed to create a sampled signal that can identify physical conditions in the real world and are then assigned to the necessary users [9–11]. Figure 1 depicts the application scenarios for UAVs. For instance, in agricultural production, a UAV based on the blockchain in 6G wireless communications could extract soil features more precisely, providing guidance and prospects for agricultural professionals to make decisions. Meanwhile, in terms of precise measurement and fertilization, UAVs can also carry out more accurate assessments of crop quality [12] due to their high reliability and connectivity. Drones are already being used to address coronavirus disease 2019 (COVID-19), assisting in the monitoring of people's temperatures, heart and respiratory rates, monitoring and controlling social distancing in public places, and delivering supplies to infected people under quarantine. Robots and UAVs with thermal imaging systems are already widely used and have contributed significantly to minimizing the spread of COVID-19. Drones are anticipated to play a larger role in medical supply and rescue operations following the implementation of blockchain technology and 6G wireless network platforms in the future [13]. UAVs are also regularly employed and effectively interoperated in military operations to gather information, move equipment, conduct surveillance and reconnaissance, and launch direct attacks when weaponized. If applied in the 6G network, UAV communication could provide a higher quality of service under the guarantee of increased coverage areas with a larger data bandwidth, making tasks smoother.

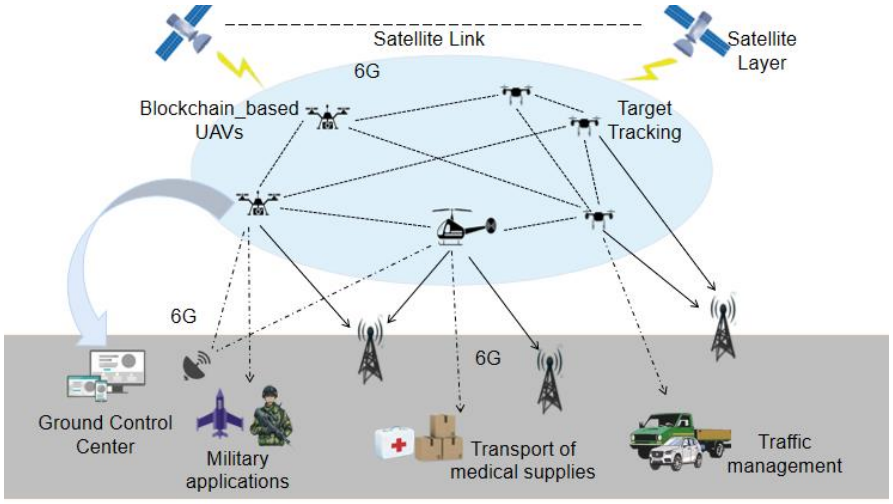

Figure 1. Diverse application scenarios of 6G and blockchain-based UAV communication.

The use of drones is significantly advancing communication systems to assist humans in various fields. However, applying blockchain-assisted UAV communication in 6G networks will also create new challenges. UAVs have many advantages that make them suitable for covert operations, such as speed, capacity, unpredictability, strength, power, and durability. Their areas of operation are often considered dangerous and beyond the reach of humans. Thus, they present a threat to social security systems and the drone communication network, which would be destroyed if UAVs carrying bombs and poisonous materials unexpectedly broke into a public area or attacked a network of routinely operating drone swarms, causing significant harm and loss. Privacy issues will also emerge if drones spend a lot of time in restricted locations and facilities, with the potential for spying on personnel or engaging in unlawful mapping activities [14,15]. At the same time, in the face of the massive amount of data generated in the 6G mobile communication network, more UAVs are required to form complex networks to achieve the planned data transmission trajectories. The number of UAVs has rapidly increased as a result of their widespread use, and their trajectories are intricate and unstable. Maintaining the communication link for UAV tracking becomes difficult to resolve when UAVs receive rapid requests, move often to gather data, or hover to provide service. Consequently, it is of great significance to detect,

track, intercept, and even destroy flying UAV targets to maintain the safety of low-altitude airspace. Thus, effective detection and tracking provide an important foundation for drone regulation.

1.2. Related Work

1.2.1. UAV Management

As technological capabilities advance, the production and deployment of UAVs will continue to expand. According to projections by the Federal Aviation Administration (FAA), the commercial drone fleet will reach 1.6 million by 2024. Therefore, in order to manage UAV operations and flight plans while carefully coordinating their locations within the airspace, rigorous protocols are required. The major aviation agencies of the globe have come together to create a system for efficiently, safely, and automatically handling UAV air traffic management (UTM), preventing a large number of drones from flying at random without reliable location tracking [16]. However, the existing UTM still has a lot of limitations as it is in its infancy and has not fully considered autonomous UAVs.

Locating a UAV is a crucial first step in tracking and positioning it. Typically, drones must be registered, just like large aircraft. For example, the FAA mandates that all drones heavier than 0.55 pounds must be numbered, equipped with a registration ID, and support a remote ID [17]. This method is limited by the fact that the form of remote ID currently required is a regular broadcast beacon transmitted over WIFI or Bluetooth, which is broadcasted over unlicensed frequency bands and cannot be guaranteed in crowded urban environments. The equipment used to receive the broadcast also has certain requirements. Consequently, further research on low-altitude target monitoring technology is urgent for the sake of national economic development and social stability and security.

Craye et al. [18] applied optical technologies to detect drones. They located potential targets through a U-Net network, then used the image classification network Res-Net to distinguish drones from interference. Finally, the space-time tracking method was employed to filter out the remaining false positives to improve detection performance. Anwar et al. [19] used acoustic technology to extract the features of UAV sounds from various environmental sounds and then classified them through support vector machine (SVM) to realize the identification and detection of UAVs. Liu et al. [20] used the pan, tilt, and zoom camera (PTZ) platform to track UAVs, obtained the trajectory, and then adopted the trained convolution neural network image data set to classify the UAV and interference. This process reduced false positives and improved system stability.

The majority of these techniques are constrained by the detection of small targets at a relatively long distance. At the same time, due to the influence of severe weather, such as thunderstorm haze, clutter interference can create serious "frame loss" issues during the tracking process, resulting in target loss. Aiming at the problem of unstable detection performance caused by the influence of clutter, such as birds, in the process of UAV tracking, this paper uses radar detection to propose a remote UAV detection method based on traditional Gaussian mixture probability hypothesis density (GM-PHD) filter. Machine learning is also employed to enhance the filter's overall effectiveness to enable the detection and tracking of UAV targets and reduce false alarms caused by clutter.

1.2.2. Target Tracking

Radar research has historically focused heavily on mobile target tracking [21,22]. Target tracking is typically defined as the process of calculating the spatial coordinates, velocity, acceleration, and other state information of the target in real time by analyzing and processing the measured value of the target that is collected by the sensor. The target tracking process is exceedingly difficult due to the uncertainty of measurement, detection, and data association and is essential to military operations, commercial services, human livelihood, and civilian sectors. The mathematician Wiener proposed the Wiener filtering method in the 1930s, which pioneered signal filtering. He assumed that the input information was a generalized stationary stochastic process with known statistical properties and

estimated the state at the current moment using measurements at all historical moments. After the 1960s, Kalman et al. used the state model to describe the covariance parameters in the Wiener filter, estimated the state through the recursive process of prediction and update, and formulated the Kalman filter (KF), a classical method of single-target tracking. The filter effect will diminish if a target is maneuvering. There are primarily two types of methods for tracking maneuverable targets: algorithm-based detection and adaptive tracking. The interaction multiple model (IMM) is an adaptive tracking algorithm that has strong scalability and is simple to combine with other algorithms [23].

With the development of technology, single-target tracking can no longer meet the needs of the military and civilians. As such, multi-target tracking (MTT) has been the subject of extensive research as an upgrade to single-target tracking and is the focus of this paper. In general, the traditional multi-target tracker consists of two steps: data association and filtering. Data association is a key technology that primarily refers to a comparison of the observed values obtained at the current moment with different targets at the previous moment. It also includes the matching of measurement and tracking through the data association algorithm, which is transformed into a single target problem to carry out MTT. In relatively perfect tracking conditions, e.g., when there is a known number of targets or a high signal-to-noise ratio (SNR), the classical data association algorithms can produce good tracking outcomes [24,25]. However, when the observed environment is more focused or has a large amount of false alarm clutter, this type of method will experience issues, resulting in NP-hardness and combinatorial explosion features that increase the computational complexity exponentially. How to reduce computation and enhance real-time performance is the key research content of MTT.

At the beginning of the 21st century, Dr. Ronald Mahler of the Lockheed Martin Institute in the United States proposed a rigorous theoretical framework to integrate expert systems theory and point processing under random set theory (RST). It was characterized by a randomly distributed set of points, as well as a randomly distributed and disordered point inside the set. Mahler applied Bayes filtering theory to the actual scene and simultaneously solved problems of complex combination and overweight computational load by creating a pure probability theory that could address most of the multi-sensor and multi-target information fusion and unification problems. He simplified the complex MTT problem and provided a new solution direction for multi-target tracking in complex airspace scenes by using finite set statistics (FISST) to enable Bayes estimates of multiple targets under numerous sensors [26]. Random set theory mostly referred to FISST. However, it remained challenging to obtain the ideal solution using Mahler's methodology because the recursive process of multi-target Bayes estimation called for multi-dimensional set integration. In order to move the estimator from theory to application, Mahler devised a probability hypothesis density (PHD) filter to transfer the posterior strength $D_k(\cdot \left| Z^k \right.)$ of the target random finite set (RFS). This filter operated by modeling the quantity and state randomness of the measurement and target so as to avoid the initial complex data association calculation. The purpose of the time variable of the target could be estimated online, thereby avoiding the complexity of data association between the observation and the station [27]. However, the issue of functions based on RFS containing a lot of integrals remained. Practical engineering applications will encounter challenges as a result of this problem's high computational complexity. Early in the 21st century, Ba-Ngu Vo and colleagues designed the GM-PHD filter, which was employed to solve the PHD recursive equation under the assumption that the target embryonic state was linear Gaussian [28]. This scheme effectively lowered processing, made it simple to extract the goal state, and increased the possibility of engineering realization. Since then, the PHD filter has been constantly improved. Our proposed algorithm based on RFS lays a unified theoretical foundation for problems, including target detection, tracking, and recognition, as well as multi-sensor data fusion, and is useful in both military and civilian settings.

In summary, RST can establish multi-target states and multi-target measurements as a RFS with sets of target states and numbers that are random and disordered. This paper

investigates the application of multi-UAVs in various 6G complex scenarios. Light and small UAVs can establish an aerial UAV platform through self-organizing networks as a part of wireless communication networks. The collecting and tracking of UAV number status information are crucial for the implementation of air-space-ground integration. In addition, it is unknown how many uncooperative UAVs pose a threat, and their detection and tracking are challenging due to high levels of randomness. According to our results, every UAV in these scenes complies with RFS and can be tracked with the RFS method.

We present a UAV tracking scheme to simplify the data complexity by using Bayes one-step recursion of random finite sets [29–31]. A DGM-PHD filter is simultaneously put forward to process the measured data, obtain the target trajectory, and realize multi-UAV target tracking in conjunction with machine learning techniques. The remainder of this article is organized as follows. Section 2 presents the system model, elaborating Bayes filtering and discussing the traditional GM-PHD filter. Section 3 introduces the algorithm in the improved DGM-PHD filter. Firstly, k-nearest neighbor (KNN) is applied to construct a target intensity estimation function to detect the emergence of UAV targets. This algorithm is then used to correlate the current state of the target with the historical trajectory, and a trajectory correlation function is constructed for the GM-PHD filter to assist in extracting the UAV motion trajectory from the filtering results. Finally, the UAV target disappearance detection algorithm is used to judge whether the target has left the monitoring range, which improves the overall tracking performance. Section 4 compares the simulation results of the two filters under the constant turning motion established in MATLAB, and optimal sub-pattern assignment (OSPA) distance evaluation is applied to assess the performance of the improved filter. According to the results, the filter is significantly enhanced and can realize the identification and tracking function of non-cooperative multi-UAV targets in future 6G complex UAV communication networks. Finally, Section 5 summarizes the work.

2. System Model

2.1. Multi-Target Bayes Filtering

In the target tracking system, sensors are used to receive the target state in real-time estimation. The Bayes filtering process can be divided into two steps. First, the known prior information is employed to predict the probability density of tracking. The current measurement value is then reused to predict the density of observation time correction to increase the credibility of the target's posterior probability density. The states in the multi-target scenario are $\left\{x_{k-1,1}, x_{k-1,2}, \cdots, x_{k-1,N_{k-1}}\right\}$, and there are N_{k-1} targets to be tested at the $k-1$-th time slot. The existing targets may then die out or continue to survive, and a new target may appear. Ultimately, the N_k new state $\left\{x_{k,1}, x_{k,2}, \cdots, x_{k,N_k}\right\}$ will be obtained. The M_k measured values $\left\{z_{k,1}, z_{k,2}, \cdots, z_{k,M_k}\right\}$ are received at the k-th time slot, and the measured information includes not only the actual target, but also clutter and false alarms. These measurements are also unordered. The problem which MTT solves is the evaluation of the number and states of targets based on the measurements of these uncertain sources.

Due to the disorder at the k-th time slot, the state and measurement of the target can be naturally expressed as a finite set:

$$X_k = \left\{x_{k,1}, x_{k,2}, \cdots, x_{k,N_k}\right\} \in F(X), \tag{1}$$

$$Z_k = \left\{z_{k,1}, z_{k,2}, \cdots, z_{k,N_k}\right\} \in F(Z). \tag{2}$$

RFS regards the target set X_k and the measurement set Z_k as the state and measurement of multi-objection, respectively. Multi-target Bayes filtering is the key to applying the RFS method to target tracking, which can recursively transfer the filtering density of multi-target states forward in time. Unlike single-target Bayes recursion, multi-target transition density $\beta_{k|k-1}(\cdot|\cdot)$ and multi-target likelihood function $g_k(\cdot|\cdot)$ can also be defined. The multi-target transition density includes the potential forms of target motion, birth, and death, while the multi-target contingency function includes the potential forms of target detection

and virtual warning. Similar to single-target Bayes, the multi-target Bayes recursion incorporates two steps: prediction and update, which transfer the filtering density π_k as follows:

$$\pi_{k|k-1}(X_k|Z_{1:k-1}) = \int \beta_{k|k-1}(X_k|X_{k-1})\pi_{k-1}(X|Z_{1:k-1})\delta X, \tag{3}$$

$$\pi_k(X_k|Z_{1:k}) = \frac{g_k(Z_k|X_k)\pi_{k|k-1}(X_k|Z_{1:k-1})}{\int g_k(Z_k|X)\pi_{k|k-1}(X|Z_{1:k-1})\delta X}, \tag{4}$$

where $\pi_{k\,|\,k-1}(X_k\,|\,Z_{1:k-1})$ denotes the multi-target prediction density at the k-th time slot, $\pi_k(X_k|Z_{1:k})$ is the multi-target posterior density at the k-th time slot, and $Z_{1:k-1}$ is the set of all measurements from the first time slot to the $k-1$-th time slots. Equations (3) and (4) change with different dimensions of X_k and Z_k at the k-th time slot, and the integrals are set integrals, so there are multiple multi-dimensional integrals in multi-target Bayes filtering. This means that a closed-form solution is generally not available. How to use multi-target Bayes recursion to obtain the target tracking solution and reduce the computation will be addressed in this paper.

2.2. Traditional GM-PHD Filter

As PHD filter makes use of multiple integrals and the general expression has no closed form, it is difficult to apply in engineering. To find a closed solution for PHD recursion, BN Vo developed a GM-PHD filter to study linear Gaussian multiple targets. The aspects included in this algorithm are discussed as follows.

2.2.1. Prior Hypothesis

To facilitate the engineering realization of PHD filter, in order to ensure the result of PHD recursion has a closed form, it is first necessary to make some assumptions for the GM-PHD filter. These include:

A1: There is no connection between different targets, which evolve independently and generate independent measurements;

A2: The clutter in the observation space is Poisson distributed, and the clutter and the measurement value generated by the target are mutually independent;

A3: The multi-target RFS derived from the multi-target prediction density $\pi_{k|k-1}$ is also a Poisson-type distribution;

A4: All the multi-objections confirm to the linear Gaussian dynamic form, and the observation form is also linear Gaussian:

$$\beta_{k|k-1}(X_k|X_{k-1}) = N\Big(x_k; F_{k|k-1}x_{k-1}, Q_{k-1}\Big), \tag{5}$$

$$g_k(Z_k|X_k) = N(z_k; H_k x_k, R_k), \tag{6}$$

where $N(\cdot; m, P)$ represents the Gaussian probability density with mean m and covariance P; $F_{k\,|\,k-1}$ is the state transition matrix; Q_{k-1} is the process noise covariance; H_k is the observation matrix; R_k is the measurement noise covariance.

A5: The target survival probability $P_{s,k}(x)$ and the target detection probability $P_{d,k}(x)$ have nothing to do with the target state:

$$P_{s,k}(x) = P_{s,k}, \tag{7}$$

$$P_{d,k}(x) = P_{d,k}. \tag{8}$$

A6: The intensity of the newly generated target can be written in a Gaussian mixture form:

$$D_{\gamma,k}(x) = \sum_{i=1}^{J_{\gamma,k}} \omega_{\gamma,k}^{(i)} N\Big(x; m_{\gamma,k}^{(i)}, P_{\gamma,k}^{(i)}\Big), \tag{9}$$

where, $J_{\gamma,k}$, $\omega_{\gamma,k}^{(i)}$, $m_{\gamma,k}^{(i)}$ and $P_{\gamma,k}^{(i)}$ are the parameters related to the intensity of target regeneration and represent the total component, weight, mean, and covariance of the i-th component of the target regeneration, respectively.

2.2.2. Forecast Update

The closed solution of the Gaussian mixture realization of PHD filtering, or the GM-PHD recursive solution, can be constructed on the premise of meeting the above assumptions. Filtering is then implemented through the prediction and update phase.

(a) Prediction process:

The survival target intensity $D_{s,k|k-1}(\boldsymbol{x})$ is given as:

$$D_{s,k|k-1}(x) = P_{s,k} \sum_{i=1}^{J_{k-1}} \omega_{k-1}^{(i)} N\left(\boldsymbol{x}; m_{s,k|k-1}^{(i)}, P_{s,k|k-1}^{(i)}\right), \tag{10}$$

where:

$$m_{s,k|k-1}^{(i)} = F_{k-1} m_{k-1}^{(i)} \tag{11}$$

$$P_{s,k|k-1}^{(i)} = F_{k-1} P_{k-1}^{(i)} F_{k-1}^{T} + Q_{k-1}. \tag{12}$$

The posterior intensity at the $k-1$-th time and the prediction intensity at the k-th time can be written in Gaussian mixture form:

$$D_{k-1}(\boldsymbol{x}) = \sum_{i=1}^{J_{k-1}} \omega_{k-1}^{(i)} N\left(\boldsymbol{x}; m_{k-1}^{(i)}, P_{k-1}^{(i)}\right), \tag{13}$$

$$D_{k|k-1}(\boldsymbol{x}) = D_{s,k|k-1}(\boldsymbol{x}) + D_{\gamma,k}(\boldsymbol{x}). \tag{14}$$

(b) Update process

According to the assumptions of A4~A6, the posterior intensity of the target at the k-th time slot can be estimated using Gaussian mixture:

$$D_k(\boldsymbol{x}) = [1 - p_{d,k}(\boldsymbol{x})] D_{k|k-1}(\boldsymbol{x}) + \sum_{z \in Z_k} D_{d,k}(\boldsymbol{x}; z), \tag{15}$$

where $[1 - p_{d,k}(\boldsymbol{x})] D_{k|k-1}(\boldsymbol{x})$ represents the missed detection item in the update process, $D_{d,k}(x; z)$ represents the detection item, and

$$D_{d,k}(\boldsymbol{x}; z) = \sum_{i=1}^{J_{k|k-1}} \omega_k^{(i)}(z) N\left(\boldsymbol{x}; m_{k,k}^{(i)}(z), P_{k,k}^{(i)}\right). \tag{16}$$

2.2.3. Trim and Estimate

The GM-PHD filter has an issue with increasing computational complexity because the number of Gaussian components continues to grow over time. The desired state should be estimated using the Gaussian mixture pruning and merging procedure, which involves removing unimportant components and merging comparable components. By pruning components with smaller weights, an approximation of the posterior intensity of the Gaussian mixture can be obtained:

$$D_k(\boldsymbol{x}) = \sum_{i=1}^{J_k} \omega_k^{(i)} N\left(\boldsymbol{x}; m_k^{(i)}, P_k^{(i)}\right). \tag{17}$$

The idea of Gaussian pruning is to discard the components whose weight is lower than the preset threshold or to maintain a certain number of parts of the maximum weight. A single Gaussian component can also roughly represent a number of close Gaussian components. The GM-PHD filter can calculate the multi-target state following the trimming process. The close Gaussian components are merged, and when the mean values of the

Gaussian components are far apart, it is the local extremum of D_k. When using the GM-PHD filter, the number of targets can be inferred according to the sum of the weights, and the components with the maximum weight of the corresponding number are extracted from the PHD as the state estimation.

3. The Improved DGM-PHD Filter Based Method

The initial prior $D_0(x_0|z_0)$ at the initial moment is required when utilizing the GM-PHD for filtering and can be derived by using the prediction equation and updating equation k in any moment of the posterior density. In addition, the filtering value from the previous moment cannot be used to construct the target's motion trajectory in a realistic manner since the filtering output of the GM-PHD filter at each instant is a disordered set, making it impossible to detect the target's membership. To address this situation, we put forward a new target intensity estimation algorithm for UAVs using KNN in machine learning. Clustering is employed in unsupervised learning to design a path extraction algorithm to achieve the goal of non-cooperative UAV target tracking in the context of random initial information, such as number, state, and location unknown situations.

3.1. New UAV Target Intensity Estimation Algorithm

The detection of non-cooperative UAVs in the 6G complex situation under study in this work is unpredictable. The initial information of non-cooperative UAV targets to be tracked is entirely random, and the initial priors cannot be obtained from experience. In view of this situation, in order to use the GM-PHD filter for accurate tracking, it is necessary to identify newborn targets in the space in real time and record their initial position and state. Specifically, it is necessary to properly estimate the intensity function of newborn UAV targets, which is a crucial requirement for effective tracking with the GM-PHD filter. The KNN, which is a basic classification and regression method, determines the dependent division of new data by comparing the new data to be classified with the training sample set whose data features and categories are known.

The possible location and number of new goals can be estimated using the new goal judgment algorithm. Once the information is obtained, the corresponding value of the new goal intensity function can be updated. During the filter tracking process, the nascent target intensity is updated every three frames and then brought into the GM-PHD filter for filter tracking. The measurement data of three consecutive moments are used by KNN to detect whether there is a newborn UAV target [32]. If it is detected, the newborn intensity function of the target $D_0(x_0|z_0)$ is updated and then input into the GM-PHD filter as a prior for subsequent processing so as to ensure the real-time tracking of multiple UAVs. The basic steps of the new UAV target strength estimation algorithm based on KNN are as follows:

1. Set the measured values at time k, $k-1$, and $k-2$. Denote $d_{k,i}$ as the i-th measured value at time k, $i = 1, 2, \ldots, M$ (there are M measured values at this time); denote $d_{k-1,j}$ as the j-th measured value at time $k-1$, $j = 1, 2, \ldots, N$ (there are N measured values at this time); denote $d_{k-2,p}$ as the p-th measured value at time $k-2$, $p = 1, 2, \ldots, Q$ (there are Q measured values at this time).

2. By representing the position in two-dimensional coordinates $d = (x, y)$ and using T to represent the radar scanning period, the inter-frame distance of any measured value during the continuous filtering cycle can be calculated, and the following can be obtained:

$$\begin{cases} R_{1,ji} = \left| \frac{d_{(k-1,j)} - d_{(k,i)}}{T} \right|, \\ R_{1,pj} = \left| \frac{d_{(k-2,p)} - d_{(k-1,j)}}{T} \right|, \\ R_2 = \left| \frac{d_{(k-2,p)} - d_{(k-1,j)}}{T^2} - \frac{d_{(k-1,j)} - d_{(k,i)}}{T^2} \right|. \end{cases} \tag{18}$$

3. Find the nearest neighbor point that meets the constraint conditions of the following equation. If it meets the constraint conditions, $\left(d^*_{k-2,p}, d^*_{k-1,j}, d^*_{k,i}\right)$ can be considered as the candidate appearance target, where $d^*_{k,i}$ is the appearance position of the target:

$$R_{1,ji} \in [v_{min}, v_{max}] \&\& R_{1,pj} \in [v_{min}, v_{max}] \&\& R_2 \in [0, a_{max}]. \quad (19)$$

For the above equation, $v_{min}, v_{max}, a_{max}$ are the minimum rate, maximum rate, and maximum acceleration of the UAV target, respectively. The key to the effectiveness of the algorithm is the selection of the above threshold. If the threshold is set to be relatively small, it will be difficult to detect the target, resulting in a missed alarm. Conversely, if the threshold is relatively large, the clutter or other targets can easily be misjudged as UAV targets, resulting in a false alarm. The threshold value can be obtained by prior knowledge and is shown in the parameter table below.

4. For all alternative tracks $\left(d^*_{k-2,p}, d^*_{k-1,j}, d^*_{k,i}\right)$ in the previous step and tracks exiting at time $k-1$ $t_{k-1,s}$, if the following conditions are met $| d_{k-1,j} - t_{k-1,s} | > e$.

5. Calculate and update the nascent target intensity function and input it into the GM-PHD filter.

3.2. Target Trajectory Extraction Algorithm

When PHD filter is used for multi-UAV target tracking, the filter output at each moment is an unordered set, which makes it impossible to save and record the correlation information between the outputs at different moments. As a result, it will not be possible to determine the UAV target's flight path, and target tracking will not be accomplished. The k-means algorithm in machine learning uses Euclidean distance to measure similarities between sample points [33], which can group related items more quickly and with less computing power. The prediction update recursion of the GM-PHD filter applies k-means clustering, forming an improved DGM-PHD filter. The DGM-PHD filter can cluster the filtering results at each moment to enhance and extract the flight path of the UAV. The specific algorithm steps are as follows:

1. Input the set of S trajectory values existing at time $k-1$ $E_{k-1} = \{e_{s,k-1}\}$, $s = 1, 2, 3, \ldots, n$ and the set of filtering results obtained at time k $X_k = \{x_{k,i}\}$, $i = 1, 2, 3 \ldots m$.

2. Establish the set of initial mean vector $U = \{u_i\}$, $i = 1, 2, 3, \ldots, n$, where $u_i = e_{i,k-1}$.

3. For each filter value $x_{k,j}$, calculate the Euclidean distance $r_{j,i}$ between it and all mean vectors u_i. Find the nearest value to $x_{k,j}$, where the u_i corresponding trajectory $e_{i,k-1}$ is the trajectory of $x_{k,j}$.

4. Repeat operations 2 and 3 until the algorithm results converge.

5. If there is no observed value for a certain trajectory $e_{i,k-1}$, formulate an estimate based on the data recorded at the first two moments.

6. Determine whether the existing target escapes the observation area and if a new target enters to generate a new trajectory.

7. Output the updated track set.

3.3. Out-of-Line Detection Algorithm

In the scenario considered in our study, the current filter will keep the target locked for tracking if the UAV vanishes and cannot be detected in time. The likelihood of mistaking the clutter for the target increases the likelihood of false positives, which can reduce the precision of trajectory tracking. Based on the algorithm in the preceding section, we continue to suggest that the target is considered to have vanished if it has not been measured three consecutive times in order to make sure that no observation results are generated after the target has vanished. The UAV detection algorithm is described as follows:

1. Input the trajectory set $E_k = \{e_{i,k}\}, i = 1, 2, 3, \ldots, t$, and the trajectory state matrix $W_{l\times t}$ at the k-th time slot, where W_i records the current state of the i-th trajectory $e_{i,k}$ at the k-th time slot.

2. If the value of the trajectory is 0, calculate the estimated value through the data of the first two frames: $E_i = e_{i,k-1} + (e_{i,k-1} - e_{i,k-2})$, record the general time of target disappearing, and denote as $W_i+ = 1$.

3. Repeat steps 1 and 2 until the state matrix is traversed. If $W_i \geq 3$, the i-th trajectory is confirmed to have died, $e_{i,k}$ is deleted from E_k, and W_i is deleted from $W_{l\times t}$.

4. Set up $C = C - \{e_{i,k}\}$. Remove the targets that are not within the radar monitoring range in the track, and output the updated track set C.

The intensity estimation algorithm of the nascent UAV target is integrated with the target trajectory extraction algorithm and out-of-line detection algorithm to form the overall flow chart of DGM-PHD filtering. This process is shown in Figure 2.

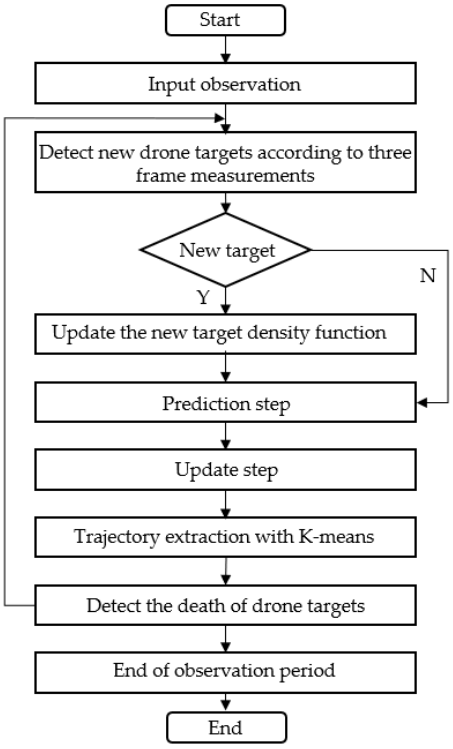

Figure 2. Overall block diagram of the DGM-PHD filter.

4. Simulation Results

4.1. Simulation Model Establishment

We display the target radar echo data on a two-dimensional plane after processing in this work. Thus, the height dimension information of the UAV can be ignored, and the target state information at each time can be reflected through the x, y two-dimensional coordinates. The position, time, and speed of the target are assumed to be random. The target state is represented as $X_k = [x, \dot{x}, y, \dot{y}]^T$, where (x, y) and $(\dot{x}, \dot{y})$ are the target location and speed information, respectively, and ϖ represents the constant angular velocity of the target in the process of rotational motion. The UAV motion satisfies the linear Gaussian model. Through mathematical deduction, the motion state and observation process are expressed by the matrix form. The constant turning motion state Equation (20) and observation Equation (21) are then formulated as follows:

$$x_k = \begin{bmatrix} 1 & \frac{\sin\omega T}{\omega} & 0 & \frac{1-\cos\omega T}{\omega} \\ 0 & -\cos\omega T & 0 & -\sin\omega T \\ 0 & \frac{1-\cos\omega T}{\omega} & 1 & \frac{\sin\omega T}{\omega} \\ 0 & \sin\omega T & 0 & \cos\omega T \end{bmatrix} x_{k-1} + \begin{bmatrix} \frac{T^2}{2} & 0 \\ T & 0 \\ 0 & \frac{T^2}{2} \\ 0 & T \end{bmatrix} v_k, \tag{20}$$

$$z_k = \begin{bmatrix} \sqrt{x_k^2 + y_k^2} \\ arctan\frac{y_k}{x_k} \end{bmatrix} + w_k, \tag{21}$$

where $V_k = [a_x(k)\ \mathrm{a}_y(k)]^T$ and $W_k = [w_x(k)\ \mathrm{w}_y(k)]^T$ are the process noise and observation noise, respectively.

MATLAB software is employed for simulation to realize radar monitoring on the two-dimensional plane, and the state space model is established through a constant turning motion of the target. The parameter settings are shown in Table 1.

Table 1. MATLAB simulation parameter settings.

Symbol	Physical Meaning	Setting Value
(x, y)	Two-dimensional monitoring range	$\begin{bmatrix} 0 & 2000 \\ -2000 & 2000 \end{bmatrix}$
T	Radar scan period	1
t	Monitoring time	100
V_k	Process noise	$\sigma_v^2 = diag([\sigma^2, \sigma^2])$
W_k	Observation noise	$\sigma_w^2 = diag([10^2, 10^2])$
p_S	Target survival probability	0.98
p_D	Target detection probability	0.98
v_{max}	Maximum movement speed of UAV	$30[\mathrm{m/s}]$
v_{min}	Minimum movement speed of UAV	$0[\mathrm{m/s}]$
a_{max}	Maximum movement acceleration of UAV	$20[\mathrm{m/s^2}]$
λ	Poisson clutter intensity	20

4.2. Simulation Experiment Results

Figure 3 depicts the real trajectories of the UAV targets with constant turning motion in the simulation observation scene. In this simulation experiment, six random UAV targets with constant turning motion were set. The trajectories of starting points and ending points were marked with different signs, and the new position and state of each target were random.

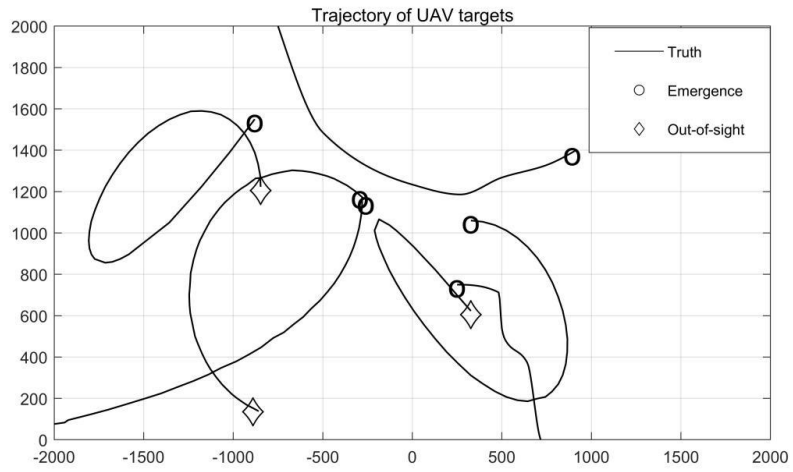

Figure 3. Real trajectories of UAVs.

In the simulation, the data of each observation time were simultaneously input into two filters for processing. The performance of the two filtering tracking schemes was then compared by controlling the consistency of other variables. Figures 4 and 5 represent the tracking results of the GM-PHD filter and the DGM-PHD filter, respectively.

It is obvious from the red marks in Figure 4 that processing by the GM-PHD filter will be interfered with by excessive clutter and generate more false alarms. The same marks are not present in the UAV target tracking scene results using the DGM-PHD filter in Figure 5. In other words, in the simulation scenario of a randomly generated, constantly turning moving UAV target, the unimproved filter can easily misidentify the UAV target and generate false alarms under increasing clutter because it lacks the ability to estimate the intensity of the nascent UAV target. The improved DGM-PHD filter incorporates a trajectory extraction algorithm based on trajectory division, which can effectively reduce false alarms to improve tracking accuracy and in turn more effectively operate in 6G complex scenes by using the data information of historical moments.

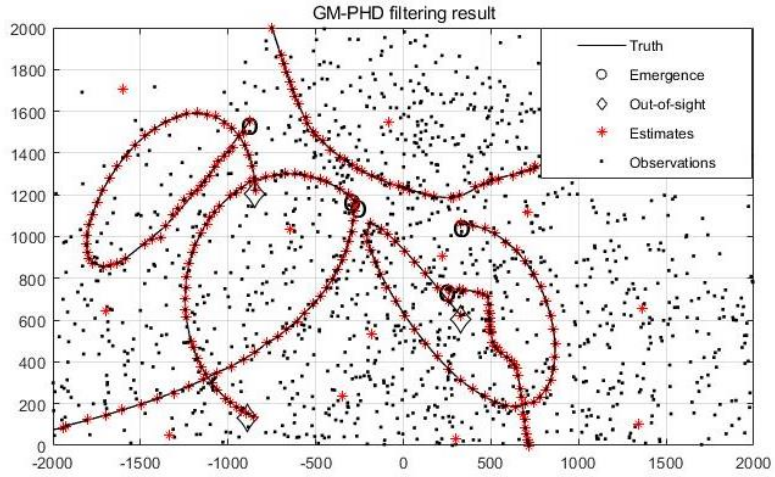

Figure 4. GM−PHD filter results.

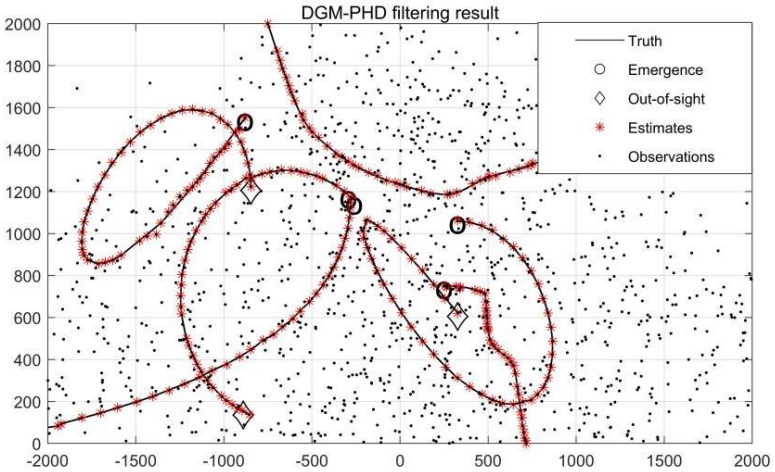

Figure 5. DGM−PHD filter results.

4.3. Performance Comparison and Evaluation

The OSPA metric is used to analyze the experimental results [34], as shown in Figure 6. Among them, OSPA Card, OSPA Loc, and OSPA Dist represent the quantity estimation, state value estimation, and comprehensive estimation errors, respectively (generally known as the OSPA distance). It can be seen that under the turning motion model, compared with the traditional GM-PHD filter, the DGM-PHD filter has a smaller OSPA distance at most

observation moments. Thus, the improved filter is more accurate than the original filter in terms of target number and target state evaluation.

Figure 7 specifically compares the estimated number of UAVs in 100 observation moments, where the solid black line represents the real number of targets, and the black dots and red circles represent the estimation of the actual number of targets by the GM-PHD filter and DGM-PHD filter, respectively. The results indicate that the DGM-PHD filter is more precise in evaluating the number of UAVs.

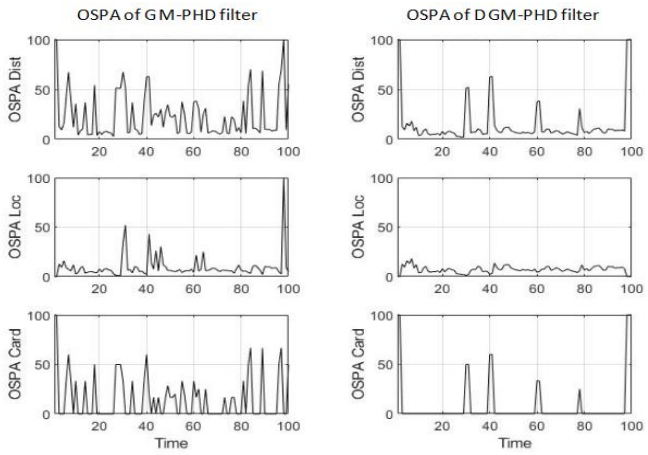

Figure 6. OSPA distance comparison.

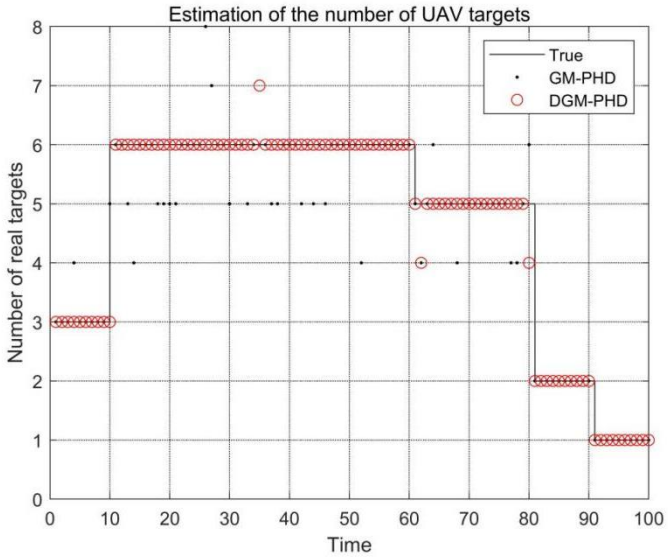

Figure 7. Comparison of estimated Number of UAV in observation Period.

The average OSPA distance between the two filters for different clutter densities is compared in Figure 8. The variation range of clutter density r is set as [0, 50], and eight UAV targets are randomly generated. As shown in Figure 8, the two schemes have a similar performance at the beginning. However, when the clutter density increases, the GM_PHD method's error increases sharply, while the error of the DGM_PHD algorithm remains stable to a certain extent. This result indicates that the improved filter can eliminate the spurious trajectory generated by transient clutter and improve the tracking performance.

The DGM-PHD filter can achieve the trajectory tracking of UAVs in conditions of high-density clutter by clustering the filtering results and using historical data to eliminate false alarms. As such, it is more effective than the traditional GM-PHD filter.

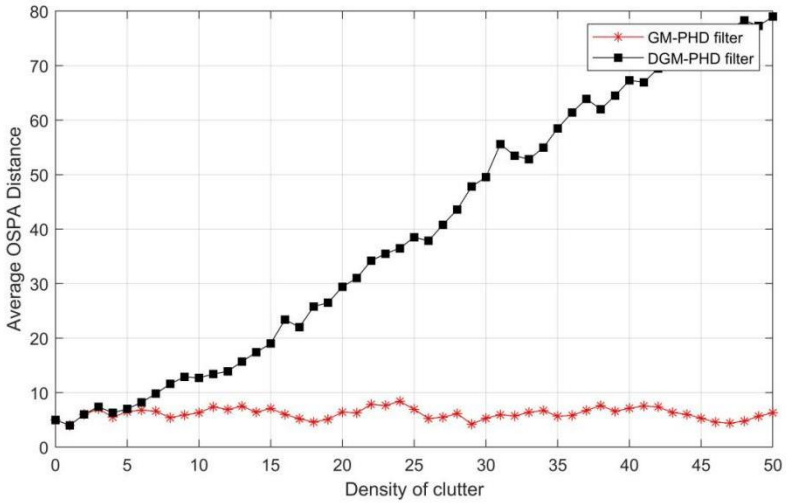

Figure 8. Average OSPA distance of the two filters with the increase of clutter density.

5. Conclusions

UAVs will play a key role in the coming 6G era and will provide additional economic benefits in blockchain networks. However, an increasing number of UAVs will also create security risks in both military and public spaces. Based on traditional GM-PHD filtering, this paper presented a new target intensity estimation algorithm using KNN to realize the detection of target appearance. A measurement division algorithm using the clustering idea was employed to realize UAV trajectory extraction, and target demise was judged using the out-of-sight detection algorithm. The algorithms were integrated to design a DGM-PHD filtering scheme, realizing the identification and tracking of multiple UAVs. Simulation experiments were carried out in MATLAB using a constant turning motion model to compare and evaluate the two filters by the OSPA distance. The results indicated that the performance of the DGM-PHD filter was stable under the condition of high clutter, which greatly reduced the false alarm rate and improved tracking accuracy. In addition, the intensity of the new target could be estimated adaptively, and the trajectory map of the target to be tracked could be generated in real time by the unsupervised learning method.

The experiment results indicated that the improved DGM-PHD algorithm had more advantages and achieved better performance than the traditional GM-PHD filter for tracking multiple UAV targets in various 6G application scenarios. However, there are still some interesting problems to be addressed in the future. In principle, the improved GM-PHD filter adopted in our work is inseparable from the linear Gaussian multi-target model, which enables the survival probability and detection probability to be independent of the target state. However, the situation is more complex in real application scenarios. The target survival and detection probability have a more general form, and the UAV motion model can be a nonlinear Gaussian model with higher compatibility. As such, the extended Kalman filter (EKF) and the unscented Kalman filter (UKF) should be considered to extend the GM-PHD filter in future research. Additionally, the Doppler radar is widely used in military equipment and can effectively detect moving targets by the Doppler effect. Therefore, future work could consider how to employ the dimension information of Doppler measurements in the current tracking scheme to further improve the tracking reliability of the filtering algorithms.

Author Contributions: Writing—original draft preparation, C.Z.; writing—review and editing, T.H.; software, M.K.; validation, T.T. and Z.Z. All authors have read and agreed to the published version of the manuscript.

Funding: This research was funded by the National Natural Science Foundation of China under Grant No. 61827901 and the Central Guidance on Local Science and Technology Development Special Fund of Shenzhen City under Project No. 2021Szvup079.

Institutional Review Board Statement: Not applicable.

Informed Consent Statement: Not applicable.

Data Availability Statement: Not applicable.

Conflicts of Interest: The authors declare no conflict of interest.

References

1. Mishra, D.; Trotta, A.; Traversi, E.; Di Felice, M.; Natalizio, E. Cooperative Cellular UAV-to-Everything (C-U2X) communication based on 5G sidelink for UAV swarms. *Comput. Commun.* **2022**, *192*, 173–184. [CrossRef]
2. Kaur, J.; Khan, M.A. Sixth Generation (6G) Wireless Technology: An Overview, Vision, Challenges and Use Cases. In Proceedings of the 2022 IEEE Region 10 Symposium (TENSYMP), Mumbai, India, 1–3 July 2022.
3. Cohari, A.; Ahmad, A.B.; Rahim, R.B.A.; Supa'at, A.S.M.; Abd Razak, S.; Gismalla, M.S.M. Involvement of Surveillance Drones in Smart Cities: A Systematic Review. *IEEE Access* **2022**, *10*, 56611–56628.
4. Angjo, J.; Shayea, I.; Ergen, M.; Mohamad, H.; Alhammadi, A.; Daradkeh, Y.I. Handover Management of Drones in Future Mobile Networks: 6G Technologies. *IEEE Access* **2021**, *9*, 12803–12823. [CrossRef]
5. Burhanuddin, L.A.B.; Liu, X.N.; Deng, Y.S.; Challita, U.; Zahemszky, A. QoE Optimization for Live Video Streaming in UAV-to-UAV Communications via Deep Reinforcement Learning. *IEEE Trans. Veh. Technol.* **2022**, *71*, 5358–5370. [CrossRef]
6. Dai, H.-N.; Wu, Y.; Imran, M.; Nasser, N. Integration of Blockchain and Network Softwarization for Space-Air-Ground-Sea Integrated Networks. *IEEE Internet Things Mag.* **2022**, *5*, 166–172. [CrossRef]
7. Aggarwal, S.; Kumar, N.; Tanwar, S. Blockchain-Envisioned UAV Communication Using 6G Networks: Open Issues, Use Cases, and Future Directions. *IEEE Internet Things J.* **2021**, *8*, 5416–5441. [CrossRef]
8. Masaracchia, A. UAV-Enabled Ultra-Reliable Low-Latency Communications for 6G: A Comprehensive Survey. *IEEE Access* **2021**, *9*, 137338–137352. [CrossRef]
9. Mozaffari, M.; Lin, X.; Hayes, S. Toward 6G with Connected Sky: UAVs and Beyond. *IEEE Commun. Mag.* **2021**, *59*, 74–80. [CrossRef]
10. Dong, C. UAVs as an Intelligent Service: Boosting Edge Intelligence for Air-Ground Integrated Networks. *IEEE Netw.* **2021**, *35*, 167–175. [CrossRef]
11. New, W.K.; Leow, C.Y. Unmanned Aerial Vehicle (UAV) in Future Communication System. In Proceedings of the 2021 26th IEEE Asia-Pacific Conference on Communications (APCC), Kuala Lumpur, Malaysia, 11–13 October 2021.
12. Zawish, M. Toward On-Device AI and Blockchain for 6G-Enabled Agricultural Supply Chain Management. *IEEE Internet Things Mag.* **2022**, *5*, 160–166. [CrossRef]
13. Zuhair, M.; Patel, F.; Navapara, D.; Bhattacharya, P.; Saraswat, D. BloCoV6: A blockchain-based 6G-assisted UAV contact tracing scheme for COVID-19 pandemic. In Proceedings of the 2021 2nd International Conference on Intelligent Engineering and Management (ICIEM), London, UK, 28–30 April 2021.
14. Giray, S.M. Anatomy of unmanned aerial vehicle hijacking with signal spoofing. In Proceedings of the 2013 6th International Conference on Recent Advances in Space Technologies (RAST), Istanbul, Turkey, 12–14 June 2013.
15. Kumar, C.; Mohanty, S. Current Trends in Cyber Security for Drones. In Proceedings of the 2021 International Carnahan Conference on Security Technology (ICCST), Hatfield, UK, 11–15 October 2021.
16. Shrestha, R.; Bajracharya, R.; Kim, S. 6G Enabled Unmanned Aerial Vehicle Traffic Management: A Perspective. *IEEE Access* **2021**, *9*, 91119–91136. [CrossRef]
17. Mujumdar, O.; Celebi, H.; Guvenc, I.; Sichitiu, M.; Hwang, S.; Kang, K.-M. Use of LoRa for UAV Remote ID with Multi-User Interference and Different Spreading Factors. In Proceedings of the 2021 IEEE 93rd Vehicular Technology Conference (VTC2021-Spring), Helsinki, Finland, 25–28 April 2021.
18. Craye, C.; Ardjoune, S. Spatio-Temporal semantic segmentation for drone detection. In Proceedings of the 2019 16th IEEE International Conference on Advanced Video and Signal Based Surveillance (AVSS), Taipei, Taiwan, 18–21 September 2019.
19. Anwar, M.Z.; Kaleem, Z.; Jamalipour, A. Machine learning inspired sound-based amateur drone detection for public safety applications. *IEEE Trans. Veh. Technol.* **2019**, *68*, 2526–2534. [CrossRef]
20. Liu, Y.C.; Liao, L.C.; Wu, H. Trajectory and image-based detection and identification of UAV. *Visual Comput.* **2021**, *37*, 1769–1780. [CrossRef]
21. Mohajerin, N.; Histon, J.; Dizaji, R.; Waslander, S.L. Feature extraction and radar track classification for detecting UAVs in civillian airspace. In Proceedings of the 2014 IEEE Radar Conference (RadarCon), Cincinnati, OH, USA, 19–23 May 2014.
22. Sarikaya, T.B.; Yumus, D.; Efe, M.; Soysal, G.; Kirubarajan, T. Track Based UAV Classification Using Surveillance Radars. In Proceedings of the 2019 22nd International Conference on Information Fusion (FUSION), Ottawa, ON, Canada, 2–5 July 2019.
23. Houles, A.; Bar-Shalom, Y. Multi-sensor tracking of a maneuvering target in clutter. *IEEE Trans. Aerosp. Electron. Syst.* **1989**, *25*, 176–189. [CrossRef]
24. Blom, H.A.; Blom, E.A. Interacting multiple model joint probabilistic data association avoiding track coalescence. In Proceedings of the 41st IEEE Conference on Decision and Control, Las Vegas, NV, USA, 10–13 December 2002.
25. Blackmans. Multiple hypothesis tracking for multiple target tracking. *IEEE Aerosp. Electro. Syst. Mag.* **2004**, *19*, 5–18. [CrossRef]

26. Mahler, R.P.S. Global integrated data fusion. In Proceedings of the 7th National Symposium on Sensor Fusion, Albuquerque, NM, USA, 29 July 1994.
27. Mahler, R.P.S. Multi-target Bayes filtering via first-order multi-target moments. *IEEE Trans. Aerosp. Electron. Syst.* **2003**, *39*, 1152–1178. [CrossRef]
28. Vo, B.N.; Ma, W.K. The Gaussian mixture probability hypothesis density filter. *IEEE Trans. Signal Process.* **2006**, *54*, 4091–4104. [CrossRef]
29. Lee, J.-Y.; Kim, W.; Kim, H.J. Tracking of Multiple Targets using GM-PHD Filter with Nonlinear Measurement Model. In Proceedings of the 2018 18th International Conference on Control, Automation and Systems (ICCAS), PyeongChang, Republic of Korea, 17–20 October 2018.
30. Wang, H.; Liang, Y.; Jiang, H.; Li, Q.; Ren, Z. Multi-target GM-PHD trackers based on strong tracking cubature Kalman filter. In Proceedings of the 2020 Chinese Automation Congress (CAC), Shanghai, China, 6–8 November 2020.
31. Gallion, T.; McKinney, C.; Chakravarty, S. Pedestrian Tracker Utilizing Sensor Fusion and a Gaussian-Mixture Probability Hypothesis Density Filter. In Proceedings of the 2019 SoutheastCon, Huntsville, AL, USA, 11–14 April 2019.
32. Martínez, F.; Frías, M.P.; P'erez, M.D.; Rivera, A.J. A methodology for applying k-nearest neighbor to time series forecasting. *Artif. Intell. Rev.* **2019**, *52*, 2019–2037. [CrossRef]
33. Qi, J.; Yu, Y.; Wang, L.; Liu, J. K-Means: An Effective and Efficient K-Means Clustering Algorithm. In Proceedings of the 2016 IEEE International Conferences on Big Data and Cloud Computing (BDCloud), Social Computing and Networking (SocialCom), Sustainable Computing and Communications (SustainCom) (BDCloud-SocialCom-SustainCom), Atlanta, GA, USA, 8–10 October 2016.
34. Beard, M.; Vo, B.T.; Vo, B.N. OSPA ((2)): Using the OSPA Metric to Evaluate Multi-target Tracking Performance. In Proceedings of the 2017 International Conference on Control, Automation and Information Sciences (ICCAIS), Chiang Mai, Thailand, 31 October–3 November 2017.